material, in principle identical over the whole sample surface. We attribute this singularity, which corresponds to about 6% of the magnetization at saturation, to the collapse of the central domain in roughly half of the dots oriented antiparallel to the field direction. This switching field is expected to be most sensitive to the local parameters of the material and less sensitive to the finite size and shape of the dots. This result is due to a combination of the central position of the domain, which is far away from the edges, and the presence of the nearby alternately oriented magnetic domains, which ensure efficient screening of the edges. Close examination of the magnetization curve (Fig. 5) reveals at least two more, although weaker, jumps at lower field (reproducible under identical conditions) that can be attributed to the initial collapse of part of the outer rings. Such a distribution of jumps may result because the height of one jump depends on both the size of the domain to be reversed and the number of dots with the same configuration. Not surprisingly, after the dots have become single-domain, a further increase in the field is necessary to overcome the strong demagnetizing field near the bottoms and the tops of the dots and to completely align the moments along the field direction.

Our results demonstrate that two length scales determine the magnetic domain structures and magnetic domain reversal processes in Co dot arrays. One length scale is set by the geometry of the dots, and the other is imposed by the size of a domain wall separating two adjacent domains. When starting from a previously stabilized concentric ring configuration, we observe clear jumps in the first magnetization curve of an array that are clearly linked to specific domain annihilation processes.

Investigating domain patterns in magnetic storage devices is becoming increasingly necessary for industrial applications as written bits become smaller and smaller. In order to prevent accidental switching of magnetic domains, stringent control of the quality of the material and the dot geometry is required.

REFERENCES AND NOTES

1. G. A. Gibson and S. Schultz, *J. Appl. Phys.* **73**, 4516 (1993).
2. A. D. Kent, S. von Molnar, S. Gider, D. D. Awschalom, *ibid.* **76**, 6656 (1994).
3. J. Shi *et al.*, *Nature* **377**, 707 (1995).
4. S. Manalis *et al.*, *Appl. Phys. Lett.* **66**, 2585 (1995).
5. J. Shi, S. Gider, K. Babcock, D. D. Awschalom, *Science* **271**, 937 (1996).
6. J. P. Bucher and L. A. Bloomfield, *Int. J. Mod. Phys.* **7**, 1079 (1993).
7. *Phys. Today* **48** (1995).
8. W. Wernsdorfer *et al.*, *J. Magn. Magn. Mater.* **145**, 33 (1995).
9. F. Rousseaux *et al.*, *J. Vac. Sci. Technol. B* **13**, 2787 (1995).
10. R. M. H. New, R. F. W. Pease, R. L. White, *ibid.* **12**, 3196 (1994).
11. P. R. Krauss, P. B. Fischer, S. Y. Chou, *ibid.*, p. 3639.
12. D. R. Fredkin, T. R. Koehler, J. F. Smyth, S. Schultz, *J. Appl. Phys.* **69**, 5276 (1991).
13. The width of the domains is proportional to the square root of the thickness of the film as predicted by C. Kittel in *Phys. Rev.* **70**, 965 (1946).
14. M. Hehn, S. Padovani, K. Ounadjela, J. P. Bucher, *Phys. Rev. B*, in press.
15. C. Kooy and U. Enz, *Philips Res. Rep.* **15**, 7 (1960).
16. Y. Nakatani, Y. Uesaka, N. Hayashi, *Jpn. J. Appl. Phys.* **28**, 2485 (1989).
17. M. Seul and D. Andelman, *Science* **267**, 476 (1995) and references therein.
18. The mechanism is similar to the one described for Permalloy particles with in-plane magnetization (*12*), where the vortices move toward the center of the dot as the field is further decreased.
19. D. M. Donnet, K. M. Krishnan, Y. Yajima, *J. Phys. D* **28**, 1942 (1995).

20. We thank H. van den Berg, P. Panissod, and R. Stamps for fruitful discussions and J. Arabski, N. Bardou, E. Cambril, F. Carcenac, S. Padovani, and M. F. Ravet for technical support. Supported in part by the European Human Capital and Mobility Program.

1 February 1996; accepted 15 April 1996

Adenosine Diphosphate as an Intracellular Regulator of Insulin Secretion

C. G. Nichols,* S.-L. Shyng, A. Nestorowicz, B. Glaser, J. P. Clement IV, G. Gonzalez, L. Aguilar-Bryan, M. A. Permutt,† J. Bryan†

Adenosine triphosphate (ATP)–sensitive potassium (K_{ATP}) channels couple the cellular metabolic state to electrical activity and are a critical link between blood glucose concentration and pancreatic insulin secretion. A mutation in the second nucleotide-binding fold (NBF2) of the sulfonylurea receptor (SUR) of an individual diagnosed with persistent hyperinsulinemic hypoglycemia of infancy generated K_{ATP} channels that could be opened by diazoxide but not in response to metabolic inhibition. The hamster SUR, containing the analogous mutation, had normal ATP sensitivity, but unlike wild-type channels, inhibition by ATP was not antagonized by adenosine diphosphate (ADP). Additional mutations in NBF2 resulted in the same phenotype, whereas an equivalent mutation in NBF1 showed normal sensitivity to MgADP. Thus, by binding to SUR NBF2 and antagonizing ATP inhibition of K_{ATP} channels, intracellular MgADP may regulate insulin secretion.

Potassium channels that are ATP-sensitive are found in many types of cells and serve to couple metabolic state to electrical activity (*1*). By hyperpolarizing the cell, K_{ATP} channels limit electrical activity and hence reduce calcium entry into muscle and nerve cells. In the pancreas, they are a critical link between blood glucose concentration and insulin secretion (*1*). ATP binding can cause closure of the K_{ATP} channel, and, by antagonizing this action, MgADP causes channel opening. When glucose concentration is low, and hence glycolysis is inhibited, the fall in the intracellular concentration of ATP ([ATP]) and rise in [ADP] may combine to activate pancreatic K_{ATP} channels (*2*, *3*), resulting in hyperpolarization of the β cell, inhibition of calcium entry, and a halt in insulin secretion. The pancreatic K_{ATP} channel is encoded by the sulfonylurea receptor [SUR, a member of the ATP-binding cassette (ABC) superfamily] (*4*) and a small inward rectifier K channel (Kir6.2) subunit (*5*).

If changes in nucleotide concentrations link insulin secretion to the blood glucose concentration, then changes in the ADP or ATP sensitivity of the channel should shift the relation between insulin secretion and blood glucose concentration and lead to either a diabetic, hypoinsulinemic, or hyperinsulinemic state. Inherited mutations in SUR can cause persistent hyperinsulinemic hypoglycemia of infancy (PHHI) (*6*), a disease characterized by glucose-independent insulin secretion (*7*). We isolated mutations in SUR by analysis of genomic DNA samples from individuals affected with PHHI. In one individual, a mutation was found that corresponded to a point mutation (G1479R, where glycine is replaced by arginine at position 1479) in the second nucleotide-binding fold (NBF2) of SUR. The

C. G. Nichols* and S.-L. Shyng, Department of Cell Biology, Washington University School of Medicine, St. Louis, MO 63110, USA.
A. Nestorowicz and M. A. Permutt, Division of Metabolism and Endocrinology, Washington University School of Medicine, St. Louis, MO 63110, USA.
B. Glaser, Division of Endocrinology and Metabolism, Hadassah Medical School, Hebrew University, Jerusalem, Israel.
J. P. Clement IV, G. Gonzalez, L. Aguilar-Bryan, J. Bryan, Departments of Cell Biology and Medicine, Baylor College of Medicine, Houston, TX 77030, USA.

*To whom correspondence should be addressed. E-mail: cnichols@cellbio.wustl.edu
†These authors contributed equally to this work.

mutation is in a region (Fig. 1A) that is proposed to link nucleotide binding to the regulation of Cl^- channel activity (*8*, *9*) in the cystic fibrosis transmembrane regulator (CFTR), a related ABC cassette protein.

We constructed a G1479R mutation in the hamster SUR (haSUR) (*10*) and coexpressed wild-type or mutant SUR with Kir6.2 in COSm6 cells (*5*, *11*) (Fig. 1B). $^{86}Rb^+$ efflux measurements were then used to examine the effects of glucose deprivation and diazoxide on macroscopic channel activity (*12*). Diazoxide activates K_{ATP} channels in pancreatic β cells and has been successfully used to treat some forms of PHHI (*7*). No K_{ATP} channel activity was present in untransfected COSm6 cells or cells transfected with Kir6.2, or SUR, alone (*5*). Glibenclamide-sensitive K_{ATP} channel activity was elicited in wild-type SUR–Kir6.2 transfectants, either in response to metabolic inhibition or with the application of diazoxide (300 μM). In contrast, some K_{ATP} channel activity in mutant SUR(G1479R)–Kir6.2 transfectants could be observed with diazoxide, but no activity was activated in response to metabolic inhibition (Fig. 1B), consistent with such mutant channels in humans not activating in vivo in response to glucose deprivation, and hence causing the PHHI phenotype.

In inside-out patch-clamp experiments (*13*), the haSUR G1479R mutant channels had normal sensitivity to inhibition by ATP in the absence or presence of Mg^{2+} (Fig. 2, A and B). Diazoxide opened G1479R mutant channels in the presence of blocking concentrations of ATP, but not as effectively as it opened wild-type channels (Fig. 2C). Metabolic inhibition should lower the cytosolic [ATP], a potential physiological regulator of channel activity. These results reveal normal [ATP] sensitivity of the mutant channel and cannot explain the failure of metabolic inhibition to activate the channels. The paradox can be explained by the effect of MgADP on the channel (Fig. 3). Nucleotide diphosphates have complex actions on wild-type K_{ATP} channels (*2*, *14*, *15*). ADP^{3-}, in the absence of Mg^{2+}, causes channel inhibition as a weaker analog of ATP^{4-}. K_{ATP} channel activity declines (runs down) slowly after patch excision, and MgADP can subsequently cause a recovery of channel activity. Finally, MgADP can antagonize channel inhibition by ATP, and this action may be important in stimulating channel activity at physiological [ATP]. Mean channel activity in the absence of nucleotides, sensitivity to ADP^{3-} inhibition, and the rate of rundown after patch excision were not different between wild-type and mutant channels (*15*). However, the G1479R mutation abolished MgADP antagonism of ATP inhibition (Fig.

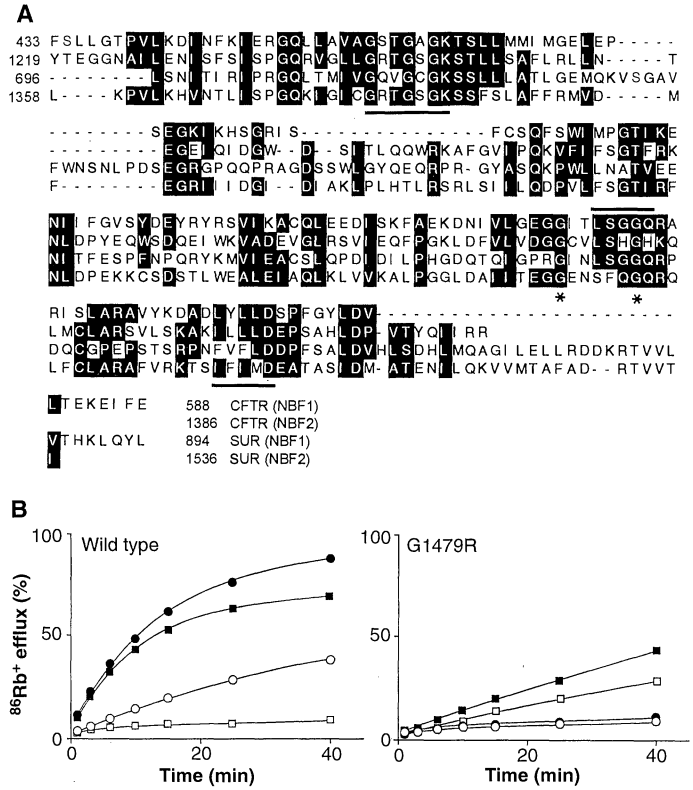

Fig. 1. A mutation in NBF2 of SUR gives rise to a PHHI phenotype. (**A**) Sequence alignments of NBF1 and NBF2 of CFTR and haSUR. Walker A and B sites are underlined. The overlined site is the proposed linker region (*9*). G827, G1479, and G1485 in SUR NBF1 and NBF2 are indicated by asterisks (*20*). Identical functional groups in three or more sequences are boxed in black. (**B**) $^{86}Rb^+$ efflux from COSm6 cells coexpressing Kir6.2 and wild-type or G1479R mutant haSUR. Graphs show efflux in the presence of metabolic inhibitors (closed circles), 300 μM diazoxide (closed squares), metabolic inhibitors plus 1 μM glibenclamide (open circles), or 300 μM diazoxide plus 1 μM glibenclamide (open squares). Abbreviations for the amino acid residues are as follows: A, Ala; C, Cys; D, Asp; E, Glu; F, Phe; G, Gly; H, His; I, Ile; K, Lys; L, Leu; M, Met; N, Asn; P, Pro; Q, Gln; R, Arg; S, Ser; T, Thr; V, Val; W, Trp; and Y, Tyr.

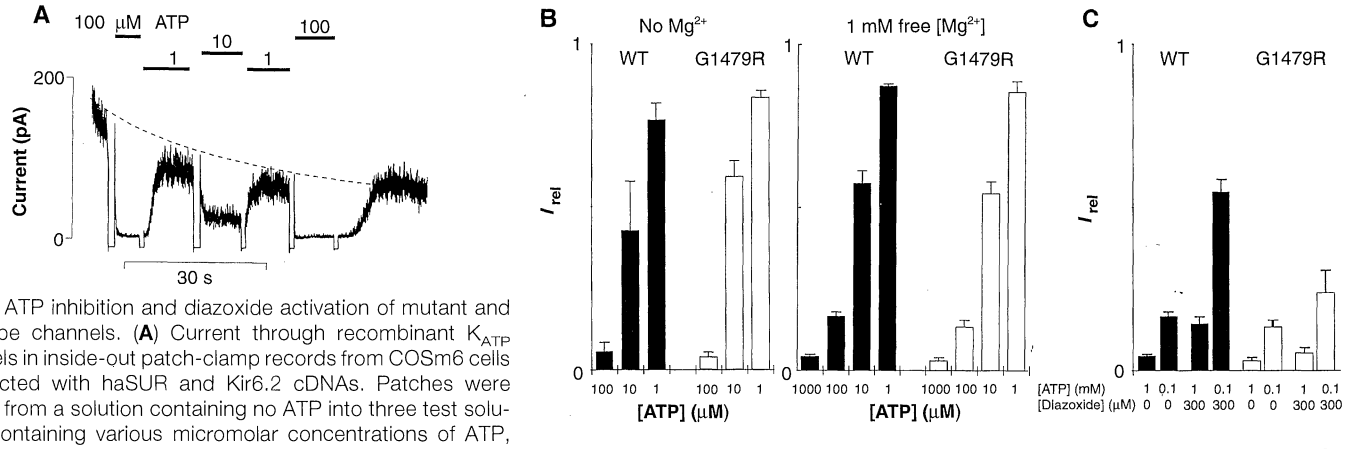

Fig. 2. ATP inhibition and diazoxide activation of mutant and wild-type channels. (**A**) Current through recombinant K_{ATP} channels in inside-out patch-clamp records from COSm6 cells transfected with haSUR and Kir6.2 cDNAs. Patches were moved from a solution containing no ATP into three test solutions containing various micromolar concentrations of ATP, and then back through each test solution to a solution without ATP. (**B**) The current for each exposure to test solution (ignoring the first 3 s) was averaged and expressed relative to the average current in the solution without ATP (I_{rel}). The bar graph shows mean ± SE (n = 3 to 4 patches in each case). Data are shown for wild-type and G1479R mutant channels in the absence of cytoplasmic Mg^{2+} (left) or the presence of 1 mM free Mg^{2+} (right). (**C**) Currents in the presence of 1 mM total Mg^{2+} and 0.1 or 1 mM ATP, with or without 300 μM diazoxide in wild-type and G1479R mutant K_{ATP} channels. The bar graph shows mean ± SE (n = 3 patches in each case).

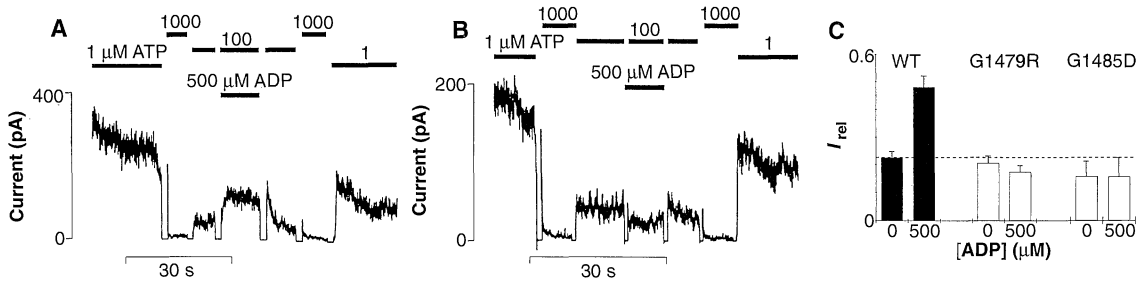

Fig. 3. MgADP activation of wild-type, but not mutant, channels. Current through (**A**) wild-type and (**B**) G1479R mutant K_{ATP} channels in inside-out patches exposed to various micromolar concentrations of ATP, or ATP with ADP. Free [Mg^{2+}] was maintained at 1 mM. (**C**) The current in 100 μM ATPrelative to the current in 1 μM ATP (I_{rel}), in the presence or absence of 500 μM ADP, for wild-type, G1479R mutant, and G1485D mutant channels (n = 3 to 6 patches in each case). Free [Mg^{2+}] was maintained at 1 mM. For all mutations, in similar experiments, the mean current in the presence of 500 μM ADP + 100 μM ATP, relative to that in 100 μM ATP alone, was 2.18 (wild type), 0.89 (G1479R), 0.98 (G1485D), 0.50 (D1506A), and 2.39 (G827D), n = 2 to 5 in each case.

3). Other Mg^{2+}-bound diphosphates, particularly MgGDP (*13*), also antagonized ATP inhibition of wild-type channels (n = 5 patches), but such stimulation was also absent in G1479R mutant channels (n = 6 patches).

ATP inhibition of K_{ATP} channel activity may require binding at two sites (*1, 2, 14, 16, 17*), and MgADP antagonism might occur through competitive binding at one site (*2, 3, 14, 16*). Our data suggest that MgADP antagonism occurs through binding in NBF2. G1479 is situated in the cytoplasmic linker region between the Walker A and B sites (*18*) of NBF2 (Fig. 1A). In *p*-glycoprotein, ADP binding occurs at NBF2 (*19*), and in CFTR, binding of ADP at this site antagonizes the stimulatory effects of ATP on CFTR Cl^- channel activity (*8*). CFTR has a glycine at the equivalent position to G1479 (G1343), and a very closely positioned glycine in NBF2 of CFTR (G1349) reduces the stimulatory effect of nucleotides on CFTR (9). We introduced a mutation to the corresponding glycine (G1485) in SUR and to the highly conserved aspartate (D1506) in the Walker B motif. G1485D and D1506A (A is alanine) produced the same phenotypic changes to the properties of expressed K_{ATP} channels as G1479R (Fig. 3). $^{86}Rb^+$ efflux was not stimulated in intact cells in response to metabolic inhibition, and in inside-out patches in the absence of Mg^{2+}, 2 mM ADP^{3-} inhibited wild-type and G1479R and G1485D mutant channels equally effectively (to 0.02, 0.01, and 0.02%, respectively, n = 3 to 6 patches). G1485D and D1506A were also fully inhibited by 1 mM ATP, suggesting that the binding of inhibitory ATP^{4-} or ADP^{3-} and transduction of the inhibitory signal are not affected by these mutations. In each case, these mutations caused loss of MgADP antagonism of ATP inhibition (Fig. 3). G1479 and G827 are at equivalent sites in NBF2 and NBF1, respectively. In contrast to the above results, G827D mutant channels were similar to wild-type channels in their sensitivity to MgADP stimulation and to inhibition by ATP (n = 3).

Our results provide direct evidence for a functional role of SUR in nucleotide regulation of K_{ATP} channel activity and suggest that the site at which MgADP stimulates K_{ATP} channels is NBF2 of SUR. They also provide direct evidence for the hypothesis (*2, 3*) that [ADP] is a physiological regulator of channel activity. We conclude that stimulation of K_{ATP} channels by MgADP is necessary for activation of K_{ATP} channels in intact β cells and, hence, that MgADP is an intracellular regulator of insulin secretion. Our findings provide a molecular explanation of the PHHI phenotype in one patient. Although the SUR mutations studied here cause a net decrease in K_{ATP} channel activity, mutations that cause an increase in K_{ATP} channel activity, such as mutations that reduce the inhibitory effect of ATP, may lead to a hypoinsulinemic, diabetic phenotype.

REFERENCES AND NOTES

1. F. M. Ashcroft, *Annu. Rev. Neurosci.* **11**, 97 (1988).
2. M. J. Dunne and O. Petersen, *FEBS Lett.* **208**, 59 (1986).
3. S. Misler, L. C. Falke, K. Gillis, M. L. McDaniel, *Proc. Natl. Acad. Sci. U.S.A.* **83**, 7119 (1986).
4. L. Aguilar-Bryan *et al.*, *Science* **268**, 423 (1995).
5. N. Inagaki *et al.*, *ibid.* **270**, 1166 (1995).
6. P. M. Thomas *et al.*, *ibid.* **268**, 426 (1995).
7. K. Zuppinger, *Prog. Pediatr. Surg.* **16**, 51 (1983).
8. M. P. Anderson and M. J. Welsh, *Science* **257**, 1701 (1992).
9. L. S. Smit, D. J. Wilkinson, M. K. Mansoura, F. S. Collins, D. C. Dawson, *Proc. Natl. Acad. Sci. U.S.A.* **90**, 9963 (1993).
10. Mutant constructs were prepared by overlap extension at the junctions of the relevant domains by sequential polymerase chain reaction (PCR). The resulting PCR products were subcloned into pECE vector [L. Ellis *et al.*, *Cell* **45**, 721 (1986)] and sequenced to verify the correct mutant construct before transfection.
11. COSm6 cells (SV40-transformed African green monkey kidney cells) were plated at a density of 2.5 × 10^5 cells per well (30-mm, six-well dishes) and cultured in Dulbecco's modified Eagle's medium plus 10 mM glucose (DMEM-HG) supplemented with fetal calf serum (FCS, 10%). The following day Kir6.2 (5 μg) and pECE-haSUR complementary DNA (cDNA) (5 μg) were cotransfected into the COSm6 cells with diethylaminoethyl dextran (5 mg/ml). Cells were incubated for 2 min in Hepes-buffered salt solution containing dimethyl sulfoxide (10%), then for 4 hours in DMEM-HG plus 2% FCS and chloroquine (100 μM), and then returned to DMEM-HG plus 10% FCS.
12. Twenty-four hours after transfection of COSm6 cells, $^{86}RbCl$ (1 μCi/ml) was added in fresh DMEM-HG containing FCS (10%), and cells were incubated for 12 to 24 hours before measurement of Rb efflux. For efflux measurements [A. S. Rajan *et al.*, *J. Biol. Chem.* **268**, 15221 (1992)], cells were incubated for 30 min at 25°C in Krebs' Ringer solution, with or without metabolic inhibitors [oligomycin (2.5 μg/ml) plus 1 mM 2-deoxy-D-glucose], glibenclamide, or diazoxide. At selected time points, the solution was aspirated from the cells and replaced with fresh solution. The $^{86}Rb^+$ in the aspirated solution was counted. Data are presented as total cellular $^{86}Rb^+$ released.
13. Patch-clamp experiments were done at room temperature in an oil-gate chamber that allowed the solution bathing the exposed surface of the isolated patch to be changed in less than 50 ms (*14*). Microelectrodes were "sealed" onto cells by applying light suction to the rear of the pipette. Inside-out patches were obtained by lifting the electrode and then passing the electrode tip through the oil gate. Membrane patches were voltage-clamped with an Axopatch 1B patch clamp (Axon, Foster City, CA). PClamp software and a Labmaster TL125 D/A converter (Axon) were used to generate voltage pulses. Data were normally filtered at 0.5 to 3 kHz, and signals were digitized at 22 kHz (Neurocorder, Neurodata, New York, NY) and stored on videotape. Experiments were replayed onto a chart recorder or digitized into a microcomputer with Axotape software (Axon). The standard bath (intracellular) solution used throughout these experiments (K-INT) had the following composition: 140 mM KCl, 10 mM K-Hepes, 1 mM K-EGTA, with additions as described. The solution pH was 7.3. The pipette solution was either also K-INT, or Na-INT, in which 140 mM KCl was replaced by 140 mM NaCl. Calculations of free [Mg^{2+}] were made with a program written by M. Kurzmak (Department of Biological Chemistry, University of Maryland), which was based on the formulations of A. Fabiato and F. Fabiato [*J. Physiol. (Paris)* **75**, 463 (1979)].
14. W. J. Lederer and C. G. Nichols *J. Physiol.* **419**, 193 (1989).
15. C. G. Nichols *et al.*, data not shown.
16. W. F. Hopkins, S. Fatherazi, B. Peter-Riesch, B. E. Corkey, D. L. Cook, *J. Membr. Biol.* **129**, 287 (1992).
17. C. G. Nichols, W. J. Lederer, M. B. Cannell, *Biophys. J.* **60**, 1164 (1991).
18. J. E. Walker, M. Saraste, M. J. Runswick, N. J. Gay, *EMBO J.* **1**, 945 (1982).
19. H. Baubichon-Cortay, L. G. Baggetto, G. Dayan, A. DiPietro, *J. Biol. Chem.* **269**, 22983 (1994).
20. We made the sequence alignments with Lasergene Megalign software (DNAStar, Madison, WI) using the Clustal method with standard weighting parameters.

21. We are grateful to A. N. Lopatin, E. N. Makhina, E. A. Wilson, and K. P. Schoor for help with experiments. Supported by grants from NIH (to C.G.N., M.A.P., and J.B.), from the Juvenile Diabetes Fund (to C.G.N. and J.B.), and from the American Diabetes Association Houston Endowment (to L.A.B.).

25 January 1996; accepted 29 March 1996